Tristability of a semiconductor laser due to time-delayed optical feedback

A. Loose,[1] B. K. Goswami,[2] H.-J. Wünsche,[1] and F. Henneberger[1]
[1]*AG Photonik, Humboldt-Universität zu Berlin, Newtonstrasse 15, 12485 Berlin, Germany*
[2]*Laser and Plasma Technology Division, Bhabha Atomic Research Centre, Mumbai 400085, India*
(Received 1 September 2008; revised manuscript received 28 January 2009; published 30 March 2009)

We present an experimental and theoretical study of multistability of a single-mode laser subject to feedback through phase tuning and amplifier sections integrated on the same chip. Closely above threshold, a regime of tristability of continuous-wave (CW) states is found for multiple ranges of amplifier and phase currents. The separation between the tristable wavelengths agrees with the channel spacing of dense wavelength multiplexing in the *C* band of optical communication making the device interesting for ternary logic applications. Complementary theoretical investigations in the framework of the paradigmatic Lang-Kobayashi model provide a consistent understanding of the experimental findings and additionally yield an analytic formula expressing the maximum number of coexisting stable CW states by the linewidth-enhancement factor α. Tristability belongs to the α range from 5 to 8 in good agreement with experiment.

DOI: 10.1103/PhysRevE.79.036211 PACS number(s): 05.45.−a, 42.55.Px, 42.79.Ta

Bistable devices, which are stable at either of two steady states, are key elements of modern computer and communication technology. More complex forms of bistability as the simultaneous coexistence of steady, periodic, or chaotic states have also been observed. One of the important fundamental queries regarding such systems is whether the number of coexisting stable states can exceed 2. This question is crucial in the context of bistability, as the coexistence of any extra state may create the possibility of sudden jump out of the binary states, even by a small intrinsic perturbation (noise). From another point of view, a multistable device is interesting on its own, e.g., as key element in higher-order logic and optical communication circuits. In particular, the design of tristable devices, such as liquid crystals [1] and optical flip-flops [2], is an active area of research.

Compared to bistability, only few experimental realizations of optical multistability have been reported, e.g., using atomic vapor in optical cavities [3]. CO_2 and doped fiber lasers under periodic parameter modulation have also shown more than two coexisting states, each either periodic or chaotic [4]. Without such periodic parameter modulation, multistability has been observed with semiconductor laser diodes either by complementing the optical devices with additional electronic circuits [5], absorptive-dispersive optical filters [6], or by splitting the resonator in two Fabry-Perot sections coupled via an air gap [7]. In this paper, we uncover a so far unknown multistable regime of a laser subject to coherent time-delayed optical feedback with features markedly different from other approaches. The experimental findings are well explained by the generic Lang-Kobayashi (LK) equations [8] when examined in the appropriate parameter range. A systematic way to increase the maximum number of coexisting states is revealed.

The experimental device is an active feedback laser (AFL) fabricated by the Fraunhofer Heinrich-Hertz-Institut (Fig. 1). It consists of a single-mode distributed feedback (DFB) laser integrated in a compound cavity with a passive phase-tuning section and an amplifier section. The device parameters agree with those of Ref. [9]. The $\lambda \approx 1537$ nm emission of the DFB laser propagates along a ridge waveguide common to all sections. Reflections at interfaces and at the antireflection (AR)-coated DFB facet are negligible, but the cleaved facet of the amplifier reflects about 30% of the incident light. The delay due to the round-trip time in the feedback sections is $\tau \approx 20$ ps. Although being extremely small, this delay plays an important role for the self-organization processes in the device [10]. Further important parameters of the feedback loop are the optical phase shift along the round trip $\varphi = \omega_0 \tau$, taken at the frequency ω_0 of the feedback-free DFB laser, and the feedback strength K as the ratio of in- and outgoing field amplitudes at the interface between the DFB laser and the passive section. For a given DFB laser current (I_d), φ and K can be independently varied over wide ranges by properly choosing the driving currents I_p and I_a for the passive and the amplifier sections, respectively. Thus, various types of feedback-related phenomena are accessible without changing the device. Exploiting this opportunity, different types of bifurcations, self-pulsations, and optical chaos have already been revealed [11] and even applied in optical data communication [12].

In all these cases, the DFB laser has been pumped well above the lasing threshold. Multistability appears in a different regime of operation when the DFB section is biased only

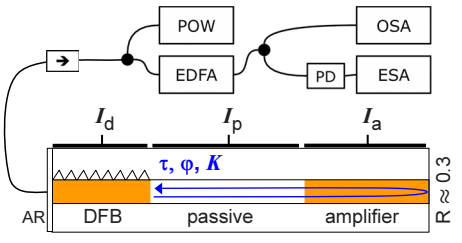

FIG. 1. (Color online) Schematic side view of the multisection device and sketch of experimental setup. DFB current I_d, phase current I_p, and amplifier current I_a are supplied with an accuracy of ± 0.05 mA. The temperature is stabilized at 20.01 ± 0.01 °C. Light emitted from the AR-coated DFB facet is coupled into a single-mode fiber and analyzed after passing an optical isolator (arrow). POW, optical power meter. EDFA, erbium doped fiber amplifier. OSA, optical spectrum analyzer (HP 71451-B). PD, u2t photodiode. ESA, electrical spectrum analyzer (Rohde & Schwarz FSP 9).

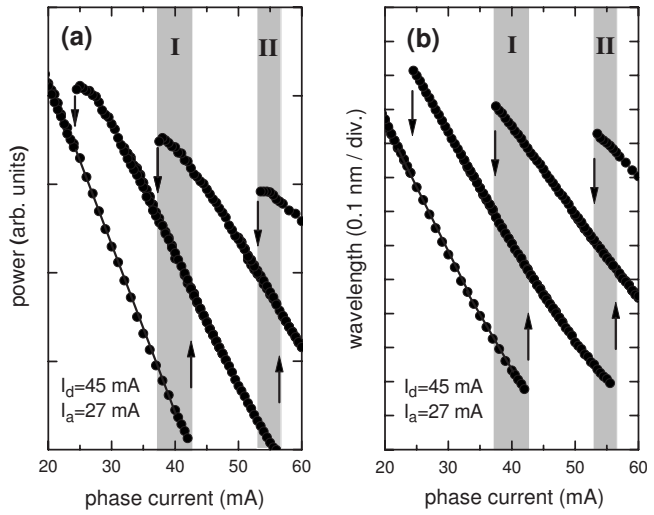

FIG. 2. (a) Power and (b) wavelength of AFL emission versus phase current I_p at I_d=45 mA and I_a=27 mA. Vertical arrows, mode jumps at the end of stable branches. Regions of tristability are shaded gray (I and II).

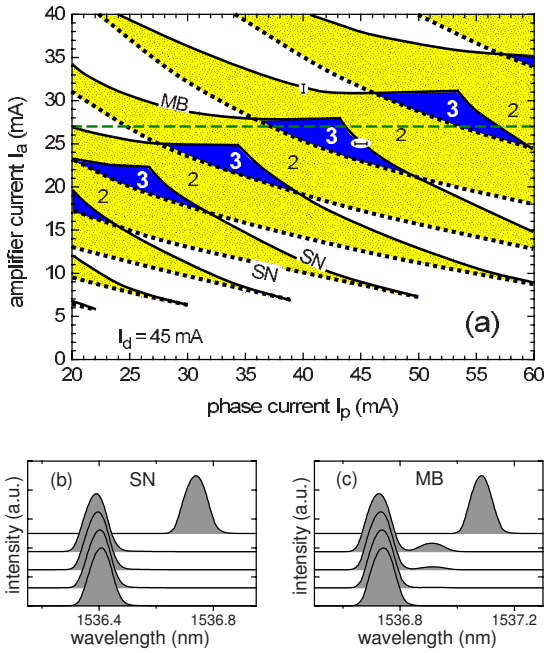

FIG. 3. (Color online) (a) Domains of multistability in the (I_p, I_a) plane. Solid lines, mode jumps forward (increasing I_a or I_p). Dotted lines, mode jumps for backward tuning. MB, mode-beating instability. SN, saddle-node bifurcation. Digits, number of coexisting stable states. Domains of bistability and tristability are dotted (yellow) and dark gray (blue), respectively. Horizontal dashed line (green), cut expanded in Fig. 2. (b) and (c) Evolution of optical spectra when crossing the SN and the MB borders along 1 mA long intervals as indicated in panel (a). Peak heights are normalized.

slightly above threshold. We consider an example where the current applied to the DFB section is only 1.5 mA higher than the threshold current I_d^{th}=43.5 mA, the amplifier current I_a is kept at 27 mA, while the phase current I_p is varied both forward and backward. Under these conditions, the laser emits continuous wave (CW), as confirmed by optical spectra (OSA) and power spectra (ESA). The emission wavelengths and powers plotted in Fig. 2 exhibit cyclic variations corresponding to roughly three 2π cycles of φ. These variations are not continuous, but appear as sequences of finite branches with negative slope. Each branch belongs to a certain optical mode of the compound cavity. At the edge of a branch, the wavelength jumps to the next mode. The different branches exhibit a considerable overlap. In particular, two regions of tristability are visible, (I) ranging from around 37 to 43 mA and (II) from around 53 to 56 mA. All coexisting states are long-time stable; no spontaneous jumps are observed within hours. No tristability is observed in other cycles at smaller or larger phase currents. Subsequent phase cycles differ slightly from each other, which can be understood as follows. The phase-tuning section is passive because its band gap exceeds the photon energy of the laser. Interband transitions are prevented this way, but free-carrier intraband absorption takes place. The latter increases with the injection level and reduces the feedback amplitude. Thus, different phase cycles are not equivalent but belong to different feedback amplitudes. We conclude that tristability appears not only in a limited range of feedback phase but also requires a certain medium strength of feedback.

The feedback strength K is adjustable by the amplifier current. In order to explore the systematics, scans of the (I_a, I_p) parameter plane were conducted. The phase and amplifier currents were tuned in steps of 0.05 mA forward and backward between 0 and 100 mA. Measured positions of mode jumps and degrees of multistability are viewed in Fig. 3(a) in a representative 60×40 mA^2 window. Several cycles of tristable islands are observed. They are equivalent to each other, i.e., their phases φ differ only by integer multiples of 2π and the estimated feedback is always around 3% of the intensity. The relatively small feedback level justifies the application of the Lang-Kobayashi model given below. The upshift of the islands with increasing I_p is, as already mentioned above, a consequence of a larger free-carrier absorption which must be compensated by a higher amplification. This scenario is stable only in a finite range of DFB currents. It starts just above threshold (43.5 mA) and ends at $I_d \approx 50$ mA. The size of the tristable islands is maximal for $I_d \approx 46$ mA.

Solid and dotted lines in Fig. 3(a) represent wavelength jumps for forward and backward current tunings, respectively. They emerge from cusps at small amplifier currents, below which no hysteresis appears. According to the model outlined below, a fold is formed in the cusp bordered by saddle-node (SN) bifurcations. With increasing feedback amplitude, the fold becomes wider and the range of bistability grows. Eventually, the width of the hysteresis exceeds one phase period and tristability appears. The widening is maximal at a kink of the upper border, beyond which it declines again. The kink indicates the touching or crossing of two bifurcations. Indeed, optical spectra differ considerably between the lines left and right from the kink. Whereas the emission keeps strictly single mode until SN, a side mode starts to grow accompanied by a mode-beating (MB) feature in the power spectrum when approaching the line labeled MB. When the side mode reaches a critical amplitude, which

is still small compared to the main mode, the emission jumps to the next branch of single-mode operation.

In what follows, we interpret the experimental findings in terms of the standard Lang-Kobayashi model [8] of delayed optical feedback. A laser under feedback with delay τ can operate in different external-cavity modes (ECMs) [13]. The lasing frequency ω and inversion N of an ECM obey the round-trip condition

$$r(\omega,N)Ke^{i\omega\tau}=1, \tag{1}$$

where $r(\omega,N)$ and $Ke^{i\omega\tau}$ are the complex amplitude reflectivities of laser and feedback cavity, respectively. The zero of $1/r$ defines the frequency ω_0 and threshold inversion N_0 of the solitary laser. Expanding $1/r$ to first order in $N-N_0$ and $\omega-\omega_0$, N can be eliminated yielding [14]

$$\Omega + C\sin\Omega = \phi. \tag{2}$$

This equation for the scaled mode frequency $\Omega=\omega\tau+\arctan\alpha$ (α: linewidth-enhancement factor) depends on only two parameters, which are related to experimental parameters as follows. $C=X\sqrt{1+\alpha^2}K\tau$ is the scaled feedback strength, where X depends on laser properties as explicitly given for Fabry-Perot and DFB lasers in Refs. [8,15], respectively. The second parameter is a phase, $\phi=\omega_0\tau+\arctan\alpha$. Note that $\varphi=\omega_0\tau$ is the zero-order phase shift along the feedback loop, which is the phase parameter tuned in experiment by sweeping the currents of feedback sections. Here, ω_0 is fixed, while $\omega_0\tau$ being of the order of 10^4 is varied by the tiny changes of τ due to the dependence of the refractive index on the injection level [16].

For $C>1$, the left-hand side of Eq. (2) varies nonmonotonically and multiple solutions Ω can exist. The number of ECMs changes by 2 in a SN bifurcation when ϕ passes an extremum [cf. Fig. 4(a)]. ECMs on increasing and decreasing parts of the left-hand side of Eq. (2) are called modes and antimodes, respectively. Antimodes are always unstable. Modes can also get unstable by various types of bifurcations (see, e.g., [13,17]). In our ultrashort-cavity case with the laser biased only slightly above threshold, a mode becomes unstable only by a Hopf bifurcation due to the existence of an antimode with the same threshold gain [10,18,19]. In Fig. 4, this instability is labeled by MB because it is usually accompanied by a characteristic mode-beating pulsation as observed in our experiments [Fig. 3(c)]. For the exemplaric case drawn in Fig. 4(a), which qualitatively resembles the experimental data of Fig. 2(b), three stable modes coexist between the SN bifurcation of the upmost mode-antimode pair (left border of the tristability domain) and the MB instability of the lowest pair (right border). Whereas the position of SN depends on C only, MB moves rightwards with rising α and reaches SN in a point of mode degeneracy when $\sqrt{1+\alpha^2}=C$ [18]. Latter case realizes the biggest possible domain of tristability for the given C. For larger α, the MB instability disappears and the domain of tristability is limited by SN bifurcations.

Domains with multiple stable ECMs in the (ϕ,C) plane are drawn in Fig. 4(b) for $\alpha=6$. The number of stable ECMs changes by 1 when crossing SN or MB curves. Only one ECM exists below the lowest SN. Two ECMs are stable in the dotted (yellow) area. Three ECMs coexist in the gray domains where areas of neighboring phase periods overlap. Figure 4(b) agrees well with the experimental findings of Fig. 3 when taking into consideration that the mapping between (I_p,I_a) and $(-\phi,C)$ is not simply linear. The mapping causes some shearing and stretching of the picture but keeps the topological relations, in particular between the regions of tristability and the kinks where MB and SN lines touch each other.

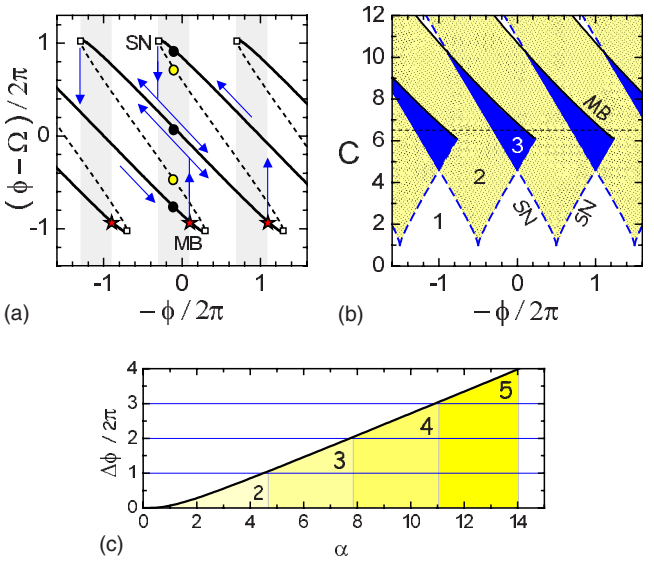

FIG. 4. (Color online) (a) Graphical representation of Eq. (2) for $C=6.5$. Vertical and horizontal axes correspond to scaled wavelength shift and phase current, respectively. Square, SN bifurcations. Circles, modes (full) and antimodes (empty). Asterisks, MB instability ($\alpha=6$). Blue arrows, central hysteresis loops. Gray shaded, domain of tristability. (b) Stationary states in the $(-\phi,C)$ plane for $\alpha=6$. Dashed (blue), SN bifurcation (of stable modes only). Solid, MB instability. Dotted (yellow) and dark gray (blue) regions, bistable and tristable domains, respectively. Thin dashed (black), cut corresponding to panel (a). (c) Fold width $\Delta\phi$ at $C=\sqrt{1+\alpha^2}$ versus α. Labels indicate the resulting maximum number of coexisting stable ECMs.

The location of SN in the $(-\phi,C)$ plane is independent of any parameter [cf. Eq. (2)] and the MB curve depends on α only [18]. The maximum degree of multistability is thus determined exclusively by α and does not depend on other parameters of the LK model. It is given by the number of modes at the MB-SN kink in Fig. 4(b). Using the coordinates of this point of mode degeneracy given in Ref. [18], the maximum number of coexisting stable ECMs is

$$M=2+\mathrm{int}\left(\frac{\Delta\phi}{2\pi}\right) \quad \text{with} \quad \Delta\phi=2[\alpha-\arctan\alpha]. \tag{3}$$

Figure 4(c) displays $\Delta\phi$ and the resulting M in dependence on α. We can expect tristability when α exceeds 5, which is the case in our device. Multistability of larger degree is expected for devices with higher α.

In conclusion, we have experimentally realized and theoretically explained multistable operation of a semiconductor laser due to delayed optical feedback. The specific configu-

ration is a multisection laser, where the feedback loop is integrated on the same chip as the DFB laser. The device is composed of individually dc-biased DFB, phase-tuning, and amplifier sections. At certain biases, the laser can emit at one of three different wavelengths, depending on how the point of operation was reached. The conditions for this so far unknown regime of tristability have been explored by systematic current variations and they are consistent with the fundamental Lang-Kobayashi model of delayed optical feedback. From the model, we can predict that even up to 4 or 5 different modes could coexist, provided the linewidth-enhancement factor α exceeds 8 and 11, respectively. Our findings may also have practical interest because the experimental laser emits in the *C* band of optical communication and the separation between the tristable wavelengths of about 0.4 nm corresponds well to the 50 GHz spacing between the channels used for dense wavelength division multiplexing.

This work was supported by the Deutsche Forschungsgemeinschaft (DFG) within the framework of Collaborative Research Centre SFB 555 and by the Department of Atomic Energy, Government of India (Contracts No. 11-R&D-BAR-4.11-0200 and No. XI-N-R&D-26.09). The authors thank Bernd Sartorius, Fraunhofer-HHI Berlin, for providing the multisection device.

[1] J. Kim, M. Yoneya, and H. Yokoyama, Nature (London) **420**, 159 (2002).
[2] K. Huybrechts *et al.*, *Winter Topical Meeting Series* (IEEE, New York, 2008), pp. 16–17.
[3] S. Cecchi, G. Giusfredi, E. Petriella, and P. Salieri, Phys. Rev. Lett. **49**, 1928 (1982).
[4] V. Chizhevsky, J. Opt B: Quantum Semiclassical Opt. **2**, 711 (2000); A. N. Pisarchik, Y. O. Barmenkov, and A. V. Kiryanov, Phys. Rev. E **68**, 066211 (2003); B. K. Goswami, Riv. Nuovo Cimento **28**, 1 (2005).
[5] M. Watanabe *et al.*, Appl. Phys. Lett. **50**, 427 (1987); J. P. Goedgebuer, A. Fischer, and H. Porte, Quantum Electron. **26**, 242 (1996); G.-Q. Xia, S.-C. Chan, and J.-M. Liu, Opt. Express **15**, 572 (2007).
[6] M. Oriá *et al.*, J. Opt. Soc. Am. B **24**, 1867 (2007).
[7] M. Ikeda, S. Oku, and M. Ogasawara, Electron. Lett. **25**, 1701 (1989).
[8] R. Lang and K. Kobayashi, IEEE J. Quantum Electron. **16**, 347 (1980).
[9] S. Bauer *et al.*, Electron. Lett. **38**, 334 (2002).
[10] O. Ushakov, S. Bauer, O. Brox, H. J. Wunsche, and F. Henneberger, Phys. Rev. Lett. **92**, 043902 (2004).
[11] O. Brox *et al.*, IEEE J. Quantum Electron. **39**, 1381 (2003); S. Bauer, O. Brox, J. Kreissl, B. Sartorius, M. Radziunas, J. Sieber, H. J. Wunsche, and F. Henneberger, Phys. Rev. E **69**, 016206 (2004); O. V. Ushakov *et al.*, EPL **79**, 30004 (2007); A. Argyris, M. Hamacher, K. E. Chlouverakis, A. Bogris, and D. Syvridis, Phys. Rev. Lett. **100**, 194101 (2008).
[12] J. Slovak *et al.*, IEEE Photonics Technol. Lett. **18**, 844 (2006); Y. A. Leem *et al.*, IEEE J. Sel. Top. Quantum Electron. **12**, 726 (2006).
[13] V. Rottschafer and B. Krauskopf, Int. J. Bifurcat. Chaos **17**, 1575 (2007).
[14] E. Patzak *et al.*, Electron. Lett. **19**, 938 (1983).
[15] F. Favre, IEEE J. Quantum Electron. **23**, 81 (1987).
[16] ϕ decreases with increasing currents. Therefore, we plot negative phases in Fig. 4 for easier comparison with the experimental data in Fig. 3.
[17] G. van Tartwijk and G. Agrawal, Prog. Quantum Electron. **22**, 43 (1998); T. Heil, I. Fischer, W. Elsasser, B. Krauskopf, K. Green, and A. Gavrielides, Phys. Rev. E **67**, 066214 (2003); A. Tabaka, M. Peil, M. Sciamanna, I. Fischer, W. Elsasser, H. Thienpont, I. Veretennicoff, and K. Panajotov, Phys. Rev. A **73**, 013810 (2006).
[18] M. Wolfrum and D. Turaev, Opt. Commun. **212**, 127 (2002).
[19] A. Tager and B. Elenkrig, IEEE J. Quantum Electron. **29**, 2886 (1993); A. Tager and K. Petermann, *ibid.* **30**, 1553 (1994); D. Pieroux *et al.*, Phys. Rev. Lett. **87**, 193901 (2001); B. Haegeman, K. Engelborghs, D. Roose, D. Pieroux, and T. Erneux, Phys. Rev. E **66**, 046216 (2002).